Aquat. Sci. 68 (2006) 1 – 15
1015-1621/06/010001-15
DOI 10.1007/s00027-005-0798-x

Aquatic Sciences

Research Article

Water clarity modeling in Lake Tahoe: Linking suspended matter characteristics to Secchi depth

Theodore J. Swift[1,4,*], Joaquim Perez-Losada[2,5], S. Geoffrey Schladow[2], John E. Reuter[3], Alan D. Jassby[3] and Charles R. Goldman[3]

[1] Department of Land, Air and Water Resources, University of California Davis, 1 Shields Avenue, Davis, California 95616, USA
[2] Department of Civil and Environmental Engineering, University of California Davis, 1 Shields Avenue, Davis, California 95616, USA
[3] Department of Environmental Sciences and Policy, University of California Davis, 1 Shields Avenue, Davis, California 95616, USA
[4] Present address: California Department of Water Resources, 901 P Street, Sacramento CA 94236, USA
[5] Present address: Departament de Fisica, Universitat de Girona, Campus de Montilivi, 17071 Girona, Catalonia, Spain

Received: 1 February 2005; revised manuscript accepted: 22 August 2005

Abstract. An additive semi-analytic model of water clarity for the forward problem of calculating apparent optical properties (AOPs) of diffuse attenuation and Secchi depth from the inherent optical properties (IOPs) due to suspended matter in oligotrophic waters is presented. The model is general in form, taking into account algal concentration, suspended inorganic sediment concentration, particle size distribution, and dissolved organic matter to predict Secchi depth and diffuse attenuation. The model's application to ultra-oligotrophic Lake Tahoe, California-Nevada, USA is described. The function of the clarity model is to quantify the relative effect of phytoplankton or phytoplankton-derived organic materials, other particles such as suspended mineral sediment, and dissolved organic matter on the lake's clarity. It is concluded that suspended inorganic sediments and phytoplanktonic algae both contribute significantly to the reduction in clarity, and that suspended particulate matter, rather than dissolved organic matter, are the dominant causes of clarity loss.

Key words. Scattering; absorption; clarity; eutrophication; erosion; oligotrophic.

Introduction

Visual clarity is an important measure of water quality, with ramifications for health and safety as well as for aesthetics. Clarity, as distinct from diffuse light attenuation, is the attenuation of visual contrast and is most commonly measured as Secchi depth. Previous attempts at clarity modeling, linking suspensoid concentrations to the inherent optical properties (IOPs) and apparent optical properties (AOPs) in freshwater systems, include Weidemann and Bannister (1986), Davies-Colley et al. (2003), Buiteveld (1995), Bukata et al. (1995), Effler and Perkins (1996), Effler et al. (2001), Hakanson, (Hakanson, 1995) and Hakanson (2003) among others. These efforts have typically addressed low clarity regimes in which the Secchi depth is less than 10 m. Larson and

* Corresponding author phone: +1 916 651 9694;
fax: +1 916 651 9653; e-mail: tswift@water.ca.gov
Published Online First: February 22, 2006

Buktenica (1998) documented the seasonal patterns of Secchi depth variations in extremely clear, ultraoligotrophic Crater Lake, Oregon. They concluded that a detailed study of the dilute particulates was key to a full understanding of Secchi depth variation.

Here we present an additive semi-analytic model of water clarity to calculate apparent optical properties (AOPs) of diffuse attenuation and Secchi depth from the inherent optical properties (IOPs) due to suspended matter in ultraoligotrophic waters (i. e., with Secchi depths in the range 15–40 m; (Carlson, 1977)). The model is general in form, taking into account algal concentration, suspended inorganic sediment concentration, particle size distribution (PSD), and colored dissolved organic matter (CDOM) concentration to predict Secchi depth and diffuse attenuation (K_d). The model captures the clarity variability in Lake Tahoe, the subject of the case study, which has seasonal variation in Secchi depth ranging from 13 m in summer to 40 m during upwelling events in winter.

In Lake Tahoe, a range of optical measurements have been taken on occasion in recent years, however, it is the near-continuous 35 year record of Secchi depth and somewhat shorter record of diffuse PAR attenuation that provide a quantitative measure of long term clarity decline. Secchi depth is a formal and specific goal of basin restoration and land-use management efforts, resulting in a need for a model link suspended matter concentrations to Secchi depth.

In an effort to reverse the trend of decreasing clarity in Lake Tahoe (Jassby et al., 1999), significant resources are being directed towards reducing nutrient and sediment fluxes into the lake and its tributaries. Water clarity as Secchi depth is one of several goals, or thresholds, driving land use management and ecosystem restoration efforts in the Tahoe basin. This model provides a linkage between dilute sediment and algae concentration and water clarity to inform decisions regarding where and how restoration efforts should be allocated for maximal effect. More generally, this model offers a tool with which to organize monitoring and research relating suspended matter to optical properties in natural waters.

Lake Tahoe is a large, deep, oligotrophic, sub-alpine lake with a mean depth of 333 m, and a maximum depth of 499 m (Gardner et al., 2000). The lake has a surface area of 501 km^2 within a watershed of 800 km^2, and a mean hydraulic residence time of 650–700 years (Marjanovic, 1989). The combination of great depth, small ratio of watershed to lake area, and granitic basin geology has produced a lake of extremely low fertility and high transparency (Jassby et al., 1994). Lake Tahoe does not freeze in winter. It is a monomictic lake and does not mix to the bottom every year. One of the most highly valued measures of Lake Tahoe's aesthetics is its clarity and deep blue color (Goldman, 2000).

When systematic measurements of water clarity began in 1968, a 20 cm diameter Secchi disk could be discerned at a depth of 31 m (annual mean); the recent annual mean is 21 m. The most recent analysis of the long-term monitoring program (with sampling at 11 day intervals) documented Secchi depth variability on seasonal, interannual, and decadal time scales (Jassby et al., 1999). Clarity is generally reduced in years with a winter of heavy snowfall, and increased in dry years. Interannual differences in mean Secchi depth can be on the order of several meters. There is also a bimodal seasonal pattern, with Secchi depth minima in approximately June and December. Analysis of the long-term data suggests that the June minimum is due to cumulative tributary discharge of suspended sediments during snowmelt while the December minimum is related to the upward mixing of phytoplankton from the deep chlorophyll maximum (40–60 m) as the thermocline degrades (Jassby et al., 1999). Episodic events, e. g., wind-driven upwelling, result in rapid changes in observed Secchi depth on the order of hours.

The model links water constituents to clarity more formally and in greater detail than previously attempted. While Secchi depth as a measure of the IOPs has certain drawbacks, it is an extremely widely used technique due to its simplicity and often is the only available optical measurement. In clear waters where the Secchi depth is many meters, its precision is comparable to or greater than that of much more sophisticated instruments, (cf. Jassby et al. 1999). The model does not rely on empirical relationships between Secchi depth and diffuse attenuation, which tend to break down if scattering and absorption do not strictly covary.

While the principles of the model can be applied to more turbid waters, e. g., Buiteveld (1995), we focus here on very clear waters. By delineating the specific scattering and absorbing roles played by pure water and of known dilute concentrations of organic particles, inorganic particles, and CDOM, it is possible to estimate the magnitude of each constituent and rank its effectiveness as an attenuant. This is in contrast to approaches that link clarity to a single surrogate such as chlorophyll concentration or total suspended solids, e. g., Tilzer (1988) or Van Duin (2001).

Model description

The optical properties of natural waters are determined by scattering and absorption of the water itself and its constituents (Mobley, 1994). Tyler (1968) and Preisendorfer (1986b), using visibility theory advanced by Duntley (1952) developed the Secchi disk relation:

$$Secchi\ Depth = \frac{\Gamma}{\langle c \rangle + \langle K_d \rangle} \quad (1)$$

where $<c>$ and $<K_d>$ are the depth-averaged beam and downwelling irradiance attenuation coefficients, respectively, and Γ is a coupling constant (Gordon and Wouters, 1978). The variables on which each of these depend are discussed further below.

The coupling constant, Γ, is a function of the eye's contrast threshold, the Secchi disk reflectivity, and water reflectivities (Gordon and Wouters, 1978; Preisendorfer, 1986b). The Secchi depth is the depth at which the contrast between the disk and the surrounding water equals the eye's contrast threshold. The contrast is affected by the band of light wavelengths of maximal transmission and the wavelength-dependency of the eye's photopic response (Dirks, 1990).

Depending on the types and concentrations of suspensoids, the band of maximal transmission will vary from lake to lake and by suspensoid types and concentrations. This maximally clear band is in the blue part of the visible spectrum for ultraoligotrophic water and shifts towards the green as suspended matter concentration increases (Davies-Colley et al., 2003; Kirk, 1994). Irradiance measurements confirm that the wavelengths of maximal transmission are in the blue part of the spectrum between 450 and 500 nm (Smith et al., 1973; Swift, 2004). Also K_d for photosynthetically available radiation (PAR) is only slightly greater than that for these most penetrating wavelengths (Davies-Colley et al., 2003, referring to Jewson et al. (1984)). Levin (2000) argues that while the minimally attenuated wavelength may vary, its effect on the relationship between beam attenuation (the major determinant of Secchi depth) and Secchi depth varies little. For the purposes of our model it is sufficient to narrow the wavelength-dependence to a quasi-monochromatic case of wavelengths around 475 nm (Gordon, 1989; Levin et al., 2000; Levin and Radomyslskaya, 2000). For application to waters of much greater suspensoid concentrations, one would have to consider the parameter values as functions of the minimally attenuated wavelength.

The beam attenuation coefficient c is the sum of the absorption and scattering coefficients a and b, respectively. The absorption term, a, is the sum of absorption by pure water, a_w, CDOM and organic (*op*) and inorganic particles (*ip*), respectively (Kirk, 1994):

$$a = a_w + a_{CDOM} + a_{op} + a_{ip} \tag{2a}$$

$$a_{op} = a^*_{Chl} \times Chla \tag{2b}$$

where a^*_{chl} is a chlorophyll-specific absorption coefficient. The values for absorption by pure water, a_w, are taken from Pope and Fry (Pope and Fry, 1997). Inorganic particles absorb weakly compared to their scattering effectiveness (Davies-Colley et al., 2003) and to the absorption by other constituents. Recent research has found that this holds for particles not containing significant amounts of iron (Babin and Stramski, 2004). Also, unpigmented organic particle (detrital) absorption correlates well with chlorophyll concentration in the case study presented here (Swift, 2004). Chlorophyll-specific absorption is also known to vary with light climate and cell physiology. These conditions must be examined for the particular water type. They are met in the case study presented here and consequently the absorption term is represented as $a_{op} = a^*_{chl} \times Chla$ where a^*_{Chla} is a chlorophyll-specific absorption, and *Chla* is the chlorophyll-a concentration.

Scattering, b, is the sum of scattering by pure water, organic particles, and inorganic particles respectively, such that $b = b_w + b_{op} + b_{ip}$. Scattering due to organic particles, or chlorophyll-covarying scattering, is parameterized using a relationship developed for chlorophyll-*a* concentration in a marine environment (Morel (1987; 1994)). Note that the scattering is due to material correlated with chlorophyll-*a*, e. g., healthy algae and covarying detritus, but not due to chlorophyll itself. Scattering by inorganic particles is represented here as the sum of the scattering of $N = 7$ particle size classes in the range of 0.5–32 µm (Eqn. 3). The use of an explicit size-differentiated spectrum of particle concentration was chosen to be more representative of scattering than bulk descriptors such as total suspended solids (TSS). We found that in Tahoe the regression of Secchi depth with TSS was significant (Jassby et al., 1999). However, a population of small (~1 µm) inorganic particles scatter light much more effectively than larger (~10 µm) particles of the same total mass, in part because of their larger number concentration and because of their higher scattering efficiency (Boss et al., 2001; Davies-Colley et al., 2003; Hutchinson and Edmondson, 1957). This yields the equation:

$$b = b_w + b^*_{chl}(Chla)^{0.62} + \sum_{n=1}^{N} f_{ip} C_n b^*_{ip_n} \tag{3}$$

where b_w is scattering by pure water (Morel, 1974), b^*_{Chla} is a chlorophyll-specific scattering coefficient, f_{ip} is the inorganic fraction of the particle population, and $b^*_{ip_n}$ is number-specific scattering by inorganic particles in size class n, of concentration C_n. *Chla*, f_{ip}, and C_n are field variables; b_w is constant and b^*_{Chla} and $b^*_{ip_n}$ are model parameters. This latter term is related to the scattering efficiency, size, and concentration of individual particles (Morel, 1994), such that

$$b_{ip_n} = C_n b^*_{ip_n} = C_n (Q_{ip_n} A_n) \tag{4}$$

where is the scattering efficiency and A_n is the projected area ($A_n = \pi D_n^2/4$), respectively, of a spherical particle

within the size class n. The scattering efficiency, Q_{ip_n}, is a particle's scattering cross-section relative to its physical cross-section, approximated by (Van De Hulst, 1957):

$$Q_{ip_n} = 2 - \frac{4}{\rho_n}\sin\rho_n + \frac{4}{\rho_n^2}(1 - \cos\rho_n) \quad (5)$$

$$\text{where } \rho_n = \frac{2\pi D_n\,(n_p - 1)}{\lambda\,/\,n_w} \quad (6)$$

is the dimensionless optical size parameter, n_p is the refractive index of the particle relative to the refractive index of water, n_w, λ is the light wavelength *in vacuo*, and D_n is the particle diameter. Q_{ip} is small for particles much smaller than λ, but rises rapidly and is approximately 2 for particles large compared to wavelength.

The inorganic fraction, f_{ip}, is defined by

$$f_{ip} = \frac{\sum_{n=1}^{N} C_n - r \times Chla}{\sum_{n=1}^{N} C_n} \quad (7)$$

where r is a conversion factor relating organic particles (algae and detritus) to measured chlorophyll-*a* concentration with units particles (mg *chla-a*)$^{-1}$. The value of r was informed by microscope counts of phytoplankton cells, elemental analysis of inorganic particles, and machine counts of total particles. The final value was determined by the genetic algorithm calibration described below. Comparison of particle size distributions within the elemental analysis samples found that, within the resolution of particle size distribution, the fraction f_{ip} was approximately constant across size classes.

K_d (Eqn. 1) is the downwelling irradiance attenuation coefficient. Kirk (1994, and references therein) found that the relation between K_d, a and b over the photic zone is given by:

$$K_d = a \times \left(\frac{\left(1 + (0.425\mu_0 - 0.19)\,\frac{b}{a}\right)^{0.5}}{\mu_0} \right) \quad (8)$$

where a and b are as defined in equations 2 and 3 and the average cosine μ_o, assuming a clear sky, is

$$\mu_0 = cos\left[sin^{-1}\left(\frac{sin(\varphi)}{1.33} \right) \right] \quad (9)$$

where φ is the solar zenith angle.

Model application: Determination of model parameters and model calibration

Methods

Methods are divided into sample collection, parameter or variable measurements, and model calibration.

Sample collection. The model development requires the following field data on each of the sampling dates: particle concentration as a function of size (C_n), elemental analysis to distinguish organic from inorganic material (f), and chlorophyll concentration (*Chla*). Samples were collected between February 1999 and December 2002 as part of the on-going UC Davis long-term monitoring program (Table 1). A total of 39 complete data sets resulted – nine from 1999, ten from 2000, six from 2001, and 14 from 2002. Water samples were collected in 10 L opaque Van Dorn bottles and stored in cold, dark conditions in acid-washed and DI-rinsed HDPE bottles. Samples used in this study were collected from depths of 0, 2, 5, 10, 15, 20, 30, and 40 m at the Index station; and at 0, 10, and 50 m at the Midlake station (Fig. 1). Measured

Table 1. Data sequence and calendar dates used for calibration and validation.

	Calibration		Validation	
Data #	Days since 1 Jan 1999	Date	Julian Date	Date
1	34	3-Feb-99	182	01-Jul-99
2	61	2-Mar-99	307	03-Nov-99
3	155	4-Jun-99	308	04-Nov-99
4	188	07-Jul-99	348	14-Dec-99
5	344	10-Dec-99	403	07-Feb-00
6	404	08-Feb-00	427	02-Mar-00
7	529	12-Jun-00	527	10-Jun-00
8	589	11-Aug-00	557	10-Jul-00
9	613	04-Sep-00	587	09-Aug-00
10	978	04-Sep-01	614	05-Sep-00
11	1006	02-Oct-01	833	12-Apr-01
12	1042	07-Nov-01	893	11-Jun-01
13	1076	11-Dec-01	1103	07-Jan-02
14	1187	01-Apr-02	1131	04-Feb-02
15	1250	03-Jun-02	1217	01-May-02
16	1278	01-Jul-02	1218	02-May-02
17	1329	21-Aug-02	1251	04-Jun-02
18	1372	03-Oct-02	1369	30-Sep-02
19	1405	05-Nov-02	1404	04-Nov-02
20	1435	05-Dec-02		

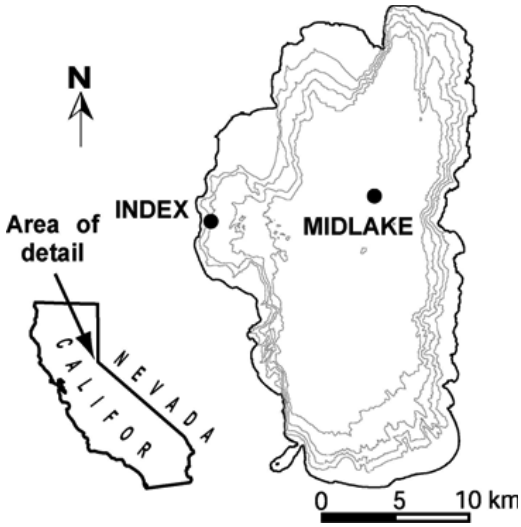

Figure 1. Map of Lake Tahoe, western United States (bathymetry contoured on 100 m intervals) and locations (•) of Midlake and Index stations. Mean depth is 313 m; maximum depth is 499 m. Midlake is lat. 39° 04.50, long. 120°00.96.

variables were trapezoidally depth-integrated from the surface to the Secchi depth. Samples listed in Table 1 represent Index and Midlake stations equally. Samples for particulate (a_p) and dissolved (a_{CDOM}) spectral absorption were collected between March 1996 and March 2000.

Chlorophyll analysis and particulate absorption. Filtration for chlorophyll analysis was performed on board or immediately afterward on shore. Chlorophyll-*a* concentration was determined by the fluorometric method (Apha, 1998) with either a Turner Designs model 10A/U or model 111 using 100 % methanol. Chlorophyll corrected for pheophytin was used in deriving the chlorophyll-specific parameters in the model.

Measurements of light absorption by organic particles, a_p, were based on the quantitative filter technique of Mitchell (1990). Filtration was performed immediately after sampling. The spectral absorbance by all matter retained on a 25 mm diameter glass-fiber filter (Whatman GF/F, 0.7 µm nominal pore size) was measured from 250 to 750 nm with a Shimadzu 150A UV-VIS spectrophotometer fitted with a quartz filter holder. After a_p measurement, the sample filter was soaked in 100 % methanol to extract pigments, followed by a measurement of the detrital, or non-pigmented particulate absorption, a_d. These measurements established that a_d covaried significantly with Chla and that at the visible wavelengths of interest (450–500 nm), a_d contributed at most approximately 35 % of total a_p. Scattering from the glass fiber filter itself acts to increase the path length of photons passing through it, thereby increasing the likelihood of absorption. This path length amplification was corrected following the suggestions of Mitchell (1990) and (Mueller and Fargion, 2002). Measurements of a_p were regressed on Chlorophyll-a concentration to derive a^*_{Chla}.

Dissolved matter absorption. Absorption by colored dissolved organic matter, a_{CDOM}, was measured by spectrophotometer using a 100 mm quartz cuvette (Mueller and Fargion, 2002). CDOM absorbance was measured in June, September, October, and November 1998 and February, April, October, and December 1999 from samples within that day's Secchi depth. Absorbance, A, was converted to absorption, a_{CDOM}, by (Kirk, 1994):

$$a_{CDOM}(\lambda) = \frac{-\ln(10) \times A(\lambda)}{pathlength,\ m} = \frac{2.303 \times A(\lambda)}{0.10} \qquad (10)$$

Due to the low concentration of CDOM in Lake Tahoe pelagic waters, the absorption at 475 nm was near the limit of detection of the spectrophotometer. Thus, the mean absorbance at 475 nm was derived from an exponential fit to the spectrum similar to Method 3 of Stedmon et al. (2000), using Igor Pro software (Wavemetrics Inc., Portland, Oregon, USA).

Particle size distribution. Individual suspended particles were counted using a Liquilaz LS-200 (Particle Measurement Systems Inc., Boulder, Colorado, USA). The LS-200 uses the principle of light scattering by individual particles. It provides number absolute concentrations of particles in 15 user selectable size bins, in the range 0.5 µm to 20 µm. This size range spans a large majority of the optically-active and most numerous suspended particles. Data from the 15 bins were combined to produce the seven particle size classes used in the optical model. To ensure accurate enumeration, samples were diluted to keep the cumulative particle count below ~ 7000 ml^{-1}. Triplicate subsamples were analyzed and averaged. Variation among sub-samples was typically 2–3 %.

The Liquilaz counts all particles whose refractive index departs from that of water sufficiently to produce a detectable scattered light signal. The Liquilaz measurements assume that the particles are spherical, with refractive index, n, of 1.59. Quartz, representative of inorganic particles, has a refractive index of ~1.54. Organic particles, whose relative refractive index is closer to that of water, may appear ~30 % smaller than true size (Knollenberg, 1987). Particles with low refractive index (e. g., unpigmented bacteria) will tend to be under-counted by the Liquilaz, both in number and size. However, by scat-

tering little, these particles are unlikely to have a large effect on clarity in the range considered here.

X-Ray Fluorescence and Scanning Electron Microscope (SEM) single particle elemental analysis. Because particle optical characteristics vary significantly due to composition (organic versus inorganic), particles were analyzed for elemental composition and size using scanning electron microscopy coupled with x-ray energy dispersive spectroscopy. Our procedures were based on Yin and Johnson (1984) and Johnson et al. (1991) as used by Coker (2000). Analysis was initiated on an International Scientific Instruments DS-130 scanning electron microscope interfaced with an Oxford ISIS 2000 EDS x-ray detector with SemiCaps imaging system. Analysis continued with an FEI-Philips XL30sFEG coupled to an EDAX Phoenix X-ray detector. Spectra were evaluated individually to classify particles.

Particles were classified based on elemental content (Johnson et al., 1991). Particles producing no elemental peaks heavier than sodium were classified as organic particles, assuming that organic particles are composed largely of carbon, nitrogen, and oxygen. Particles that had a pure silicon signal, or could be visually identified as diatoms or diatom fragments were classified as silica particles of organic origin. Particles containing silicon and typical terrestrial elements such as Aluminum, Magnesium, Titanium, or Iron were classified as inorganic particles. A sample prepared from fine stream sediment confirmed that terrestrial elements were present in approximately 90 % of particles in that sample. Thirty near-surface samples from 1999–2001 were evaluated to produce a seasonally-varying estimate of inorganic fraction.

Lake optical properties. Secchi depth was measured with a 20 cm diameter, all white disk once each month at the Midlake station and approximately every 11 days at the Index station. Secchi depth was calculated as the mean of the depth of disappearance and reappearance. The disk was viewed from the shady side of the boat to reduce surface reflectance, but clarity was always sufficiently great that the disk was fully illuminated by sunlight passing beneath the boat. Comparison of paired measurements from the sunny and shady sides of the vessel found that the difference was small, with Secchi depth viewed from the shady-side slightly greater than sunny-side.

Observed irradiance attenuation informed the bounds of the optical parameters. A Li-Cor Li-182 was used to collect vertical profiles of PAR irradiance, E_d (z, PAR), at the Index station as part of the long-term monitoring program. On several occasions, a Biospherical Instruments, Inc. MER-1012 submersible radiometer was used to measure profiles of spectral downwelling irradiance, (E_d), at 410, 441, 488, 520, 560, 630, and 683 nm, and upwelling radiance, (L_u), at 441, 488, 520, 560, and 683 nm. Diffuse downwelling attenuation, K_d, was calculated from as the depth derivative of E_d (Mobley, 1994).

Field variables

Measured chlorophyll-a concentration and particle concentrations were used as independent variables in the

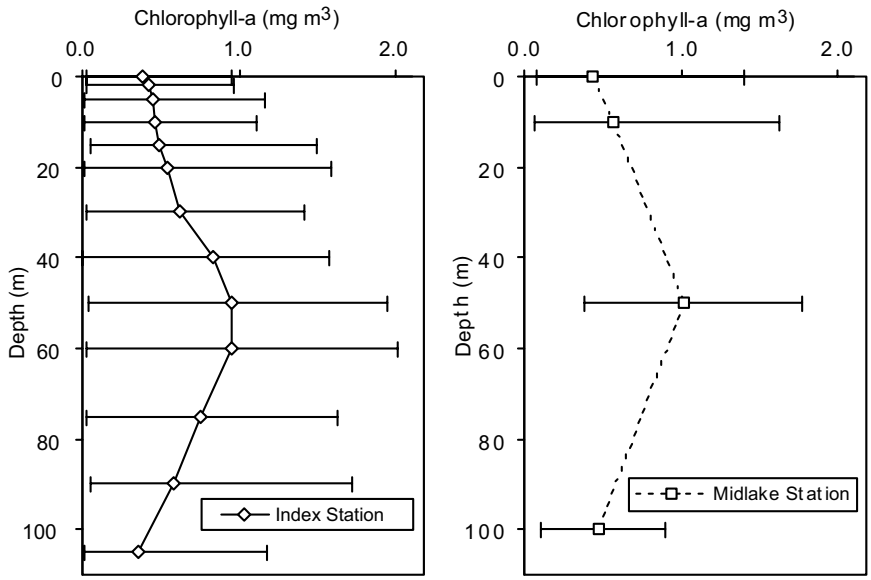

Figure 2. Vertical profiles of pheophytin-corrected chlorophyll-a concentration from (a) the Index station and (b) the Midlake station during the study period. Horizontal bars at each depth indicate the range of measurement values in the data set used.

model, with the inorganic fraction *f* determined by Equation 7. Secchi depth was the primary measurement used to evaluate goodness-of-fit of the model results. Downwelling irradiance attenuation was used as a secondary check on the overall performance of the model.

Figure 2 shows representative chlorophyll profiles for (a) the Index station (n = 26), and (b) the Midlake station (n = 31) during the study period. The bars on each measurement point show the range of values at that depth for the entire 1999–2002 calibration-validation period, using data from the long-term monitoring program. The Index station (Fig. 2a) was sampled with greater depth resolution from 0 to 105 m; n = 26. The Midlake station (Fig. 2b) was sampled at 0, 10, 50 m and thereafter every 50 m to 450 m; n = 31. Data were collected between 7 Jan 1999 and 5 Dec 2002. This includes dates in addition to those used for the calibration and validation process.

Figure 3 shows representative particle size distributions at three depths at the Index station and one depth at the Midlake station. The slope of the distribution conformed to a hyperbolic, or Junge (1963), distribution of the form , where *D* is particle diameter, *C'(D)* is the number of particles per unit volume per unit size class width ΔD, and each size class extends between *D* and *D* + Δ*D*. The hyperbolic slope is *S*, and *K* represents concentration (Mobley, 1994). *S* was similar among samples with a value of approximately 3, but the particle concentrations varied (Coker 2000, Swift 2004). For the purpose of the model the 15 measured bin sizes were transformed to an equivalent set of 7 logarithmically distributed bins (0.5–1.0, 1.0–2, 2–4, 4–8, 8–16, 16–32, 32–64 µm; Table 2). The scattering coefficient of the largest bin size (32–64 µm) was set to zero in view of the rarity of such large particles, however the bin was retained as it was required as part of a separate aggregation algorithm. The representative or mean particle diameters for each size class were calculated following Boss et al. (2001).

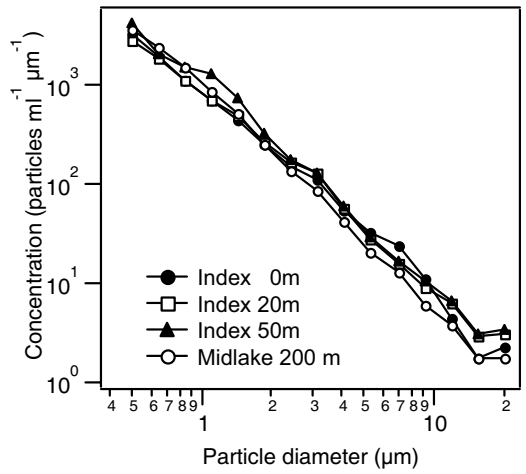

Figure 3. Representative particle size distributions measured using the full 15 particle diameter bins ranging from 0.5 to 20 µm. Samples were collected 13 Oct 1999. Note the dominance of smaller particles with respect to total particle number.

Ranges of model coefficients. As described previously, the model consists of the following coefficients: a_w, $a_{C\text{-}DOM}$, a^*_{Chla}, b_w, b^*_{Chla}, $b^*_{ip_n}$, r and Γ. A combination of measured data from Lake Tahoe, and literature values from other comparable systems was used to assign the likely range of coefficient values (Table 2).

Coupling constant, Γ. MER-1012 radiometer measurements of spectral downwelling and upwelling light were used to estimate Tahoe's spectral reflectance. Using reflectance and disk contrast threshold based on the derivation of Preisendorfer (1986), confirmed by digital analysis of disk images, Γ was set at 8.7 (Swift, 2004). This is consistent with values determined by Tyler (1968), Højerslev (1986) and Davies-Colley et al (2003).

Light absorption coefficients. Figure 4 shows representative spectra of a_p and a_{CDOM}. To derive a^*_{chl}, 48 a_p spectra from samples collected in February, April, May and December 1999 were regressed against sample chlorophyll-a concentration ($r^2 = 0.79$; $p < 0.01$), yielding $a^*_{Chla=}$(475 nm) of 0.025 m^2 mg^{-1}. This is consistent with values found in the literature (Mobley, 1994). In Figure 4, dissolved a_{CDOM}; was measured in a sample pooled from equal portions of water from 0, 10 and 20 m samples. Chlorophyll concentrations on this date were 0.21 µg Chl l^{-1} at 0 m and 0.37 µg Chl l^{-1} at 20 m. Secchi depth was 24.3 m.

While CDOM absorption was measurable in Lake Tahoe, it is a relatively small attenuant at visible wavelengths of interest for the optical model compared to the particulate constituents. Values of a_{CDOM} offshore at both the Index and Midlake stations are at the lower end of the range found in fresh waters (Kirk, 1994). CDOM absorption values are higher in the immediate vicinity of stream outflows due to tannins and humic substances from the watershed, but are substantially diluted before reaching the monitoring stations. Values of stream water a_{CDOM} were approximately ten times higher than offshore values (Swift, 2004).

The spectral absorption coefficient of pure water is still a topic of active research, e. g., Buiteveld (1994). We used absorption values for pure water (a_w) at 475 nm of 0.012 m^{-1}, found by Pope and Fry (1997).

Light scattering. Final values of b^*_{Chla} and r were found through the calibration process (see next section). The fi-

Table 2. Summary of model application: Parameter and coefficient values at 475 nm.

Parameter	Description	Value	Source
Γ	Coupling constant	8.7	Fixed [1]
a_w	Pure water absorption, m^{-1}	0.012	Fixed [2], Measured
a_{CDOM}	CDOM absorption, m^{-1}	0.038	Measured
a^*_{chl}	Chl-specific absorption, $m^2\ mg^{-1}$	0.025	Measured [3]
b_w	Pure water scattering, m^{-1}	0.0027	Fixed [4]
μ_0:	Sun angle effect on K_d	variable	Calculated [5]
$b^*_{ip_1}$ ($Q_{ipn}A_n$)	Scattering Cross-section (0.50–1.0 µm), m^2 particle^{-1}	4.287×10^{-12}	Fixed [6]
$b^*_{ip_2}$	" " (1.0–2.0 µm)	3.015×10^{-11}	Fixed
$b^*_{ip_3}$	" " (2.0–4.0 µm)	9.939×10^{-11}	Fixed
$b^*_{ip_4}$	" " (4.0–8.0 µm)	3.757×10^{-10}	Fixed
$b^*_{ip_5}$	" " (8.0–16 µm)	1.459×10^{-9}	Fixed
$b^*_{ip_6}$	" " (16–32 µm)	5.831×10^{-9}	Fixed
$b^*_{ip_7}$	" " (32–64 µm)	0	Fixed
b^*_{Chl}	Chlorophyll-specific scattering, $m^2\ mg^{-0.62}$	0.105	Calibrated [7]
r	Conversion factor for chlorophyll to particles, $m^3\ mg^{-1}$	5.6×10^9	Calibrated

Notes
1. Preisendorfer (Preisendorfer, 1986a), Gordon and Wouters (1978)
2. Pope and Fry (1997)
3. Particulate absorption measured following Mitchell (1990)
4. Morel and Prieur (1977)
6. Davies-Colley, et al. (1993), Tassan and Ferrari (1995)
5. Kirk (1994)
7. Calibration guided by Morel (1987; 1994), Kirk (1994)

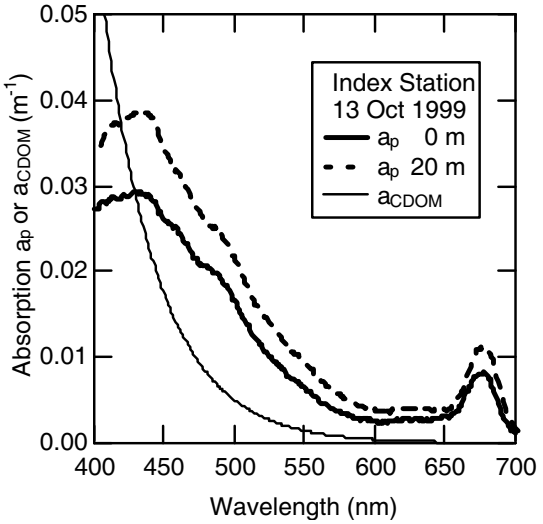

Figure 4. Representative particulate (a_p) and dissolved (a_{CDOM}) absorption spectra for near-surface samples from the Index station, collected 13 October 1999.

nal calibration value, 0.105 m^{-2} mg $Chl^{-0.62}$, is towards the lower end of the range found by Morel (1987), but similar to the range 0.05–0.12 m^{-2} mg Chl^{-1} found in Irondequoit Bay by Weidemann and Bannister (1986). Morel (1987; 1994) found $b^*_{Chla} = 0.300 \pm 0.15\ m^{-2}$ mg $Chl^{-0.62}$ for the range of chlorophyll concentrations 0.02 to >10 mg m^{-3} in marine environments. Chlorophyll-a in Lake Tahoe ranges from 0.01–3 mg Chl m^{-3} (observed mean at a representative depth of 10 m was 0.60 ± 0.26 mg Chl m^{-3} (n = 150) from 1996 to 2002). b^*_{Chla} is known to vary with, among other things, phytoplankton community structure and cell physiology. Chlorophyll-specific scattering in marine and freshwater systems range from 0.044 m^{-2} mg Chl^{-1} for *Chlamydomonas*, a chlorophyte, to 0.535 m^{-2} mg Chl^{-1} for *Skeletonema*, a marine diatom (Kirk 1994). Diatoms are often the dominant taxa in Lake Tahoe, especially during spring (Hunter et al., 1990). Weidemann and Bannister (1986) observed b^*_{Chla} in a freshwater environment to be between 0.05 and 0.10 m^{-2} mg Chl^{-1}, increasing to 0.12 m^{-2} mg Chl^{-1} for phytoplankton containing gas vacuoles. The wide range in observed specific scattering is due primarily to the differing index of refraction of cellular materials (Morel, 1987).

Tassan and Ferrari (1995) found in the laboratory setting that a suspension of very fine inorganic sediment had a scattering cross-section of 0.0011 m^2 mg^{-1}, in relatively good agreement with calculations from Mie scattering theory. Their measured particle size distribution was similar to that found at Lake Tahoe. Vant and Davies-Colley (1984), working in New Zealand lakes, also found an identical value for scattering cross-section. Assuming a bulk scattering cross-section of 0.0011 m^2 mg^{-1}, the scattering cross-section of each representative particle size was calculated by distributing this value among the seven size classes based on the Junge particle size distribution, $C_n(D)$, weighted by the scattering efficiency, . The resulting scattering coefficients for each class are presented in Table 2. For calibration purposes, the values of the seven scattering cross-sections were fixed, and *r* acted as the calibration parameter (Table 2).

Parameter calibration and model validation

Data preparation

The model depends on independent variables *Chla* and C_n, and the values of the model coefficients a_w, a_{CDOM}, a^*_{Chla}, b_w, b^*_{Chla}, b^*_{ipn}, *r* and Γ. Calibration of the model involved several steps. The available data (Chla and C_n profiles, with corresponding Secchi depth) was first checked and outliers removed. The resulting data were divided into two sets by random selection, ensuring that all seasons and years were represented. One set was used exclusively to calibrate the model, the other set was retained to validate the model. Using the calibration data set, model coefficients were examined to identify the most sensitive ones. The coefficients to which the model was relatively insensitive were fixed to either measured or literature values. Those that were the most sensitive were selected as parameters to be optimized using a genetic algorithm technique, using minimal chi-square between observed and modeled Secchi depth as the selection criterion. A Bootstrap technique was used to calculate the uncertainty associated with each parameter. For environmental data sets which involve extensive field and laboratory investment for each date, such as that involved here, calibration can be affected by the presence of outliers produced by erroneous data values (Beckman and Cook, 1983). The chi-squared function itself is sensitive to the presence of extreme points (Bevington and Robinson, 1992). A combination of a Jackknife and a rejection test was used as the basis for outlier removal (Meinrath et al., 2000). The Jackknife assesses the variation of the optimal parameter estimates by repeatedly performing the calibration omitting one data point at a time (Efron, 1979). A rejection *Q*-test of the extreme values was used as an objective criterion for discarding erroneous data (Dixon, 1950).

The maximum number of parameters that can be meaningfully developed from a data set is limited by their identifiability. Colinearity or lack of identifiability means that a change in one parameter can be compensated for by an appropriate change of other model parameters. The uncertainty ranges of the parameters, together with linear error propagation, were used to obtain a ranking of model sensitivity to parameters (Brun et al., 2002; Brun et al., 2001; Omlin et al., 2001). In linear approximation to the model equations, the global sensitivity *S* of model results to each parameter was evaluated by taking the root mean square of the error contributions of the modeled Secchi depth SD^m summed over the calibration set, *l*.:

$$S(p_k) = \left[\frac{1}{l} \times \sum_{i=1}^{l} \left(\frac{\Delta p_k}{\sigma} \times \frac{\delta SD_i^m}{\delta p_k} \right)^2 \right]^{\frac{1}{2}} \quad (11)$$

where Δp_k stands for the contribution of the uncertainty of the k-th parameter p_k, and σ is the weighting coefficient (set to 2 m in this case).

Once a meaningful set of the most sensitive model parameters were identified we used a Genetic Algorithm (GA) as an optimization technique (Beasley et al., 1993; Carroll, 1996; Goldberg, 1989; Perez-Losada, 2001). The main advantage of this technique is that it provides an automated method of converging towards the optimal set of parameter values for a given calibration data set. Sets of parameter values are evaluated (selected) by a fitness function. In this model, the chi-square provides the evaluation function between the modeled (SD^m) and observed (SD^o) Secchi depth summed over the number of calibration points, *l* :

$$\chi^2 = \sum_{i=1}^{l} \frac{(SD_i^m - SD_i^0)^2}{\sigma} \quad (12)$$

The weighting coefficient, σ, is set to 2.0 m in this application, corresponding to the hour-to-hour uncertainty in observed Secchi depth (Schladow, unpubl. data). As water sampling and Secchi depth measurement have not always coincided exactly in time (there may be 1–2 h offsets) such uncertainty is to be expected. However, even if the time gap is eliminated, there are other sources of uncertainty. Most important is the coarse spatial resolution of the available water samples. Typically only 5 samples are within the Secchi depth at the Index station, and only 2 at the Midlake station. The piecewise interpolation necessary to produce depth integrated measurements of particle and chlorophyll concentration are a large part of the uncertainty.

The predictive use of the model necessitates an accurate estimation of the model's uncertainty. Once the structure of the model is set and the parameters calibrat-

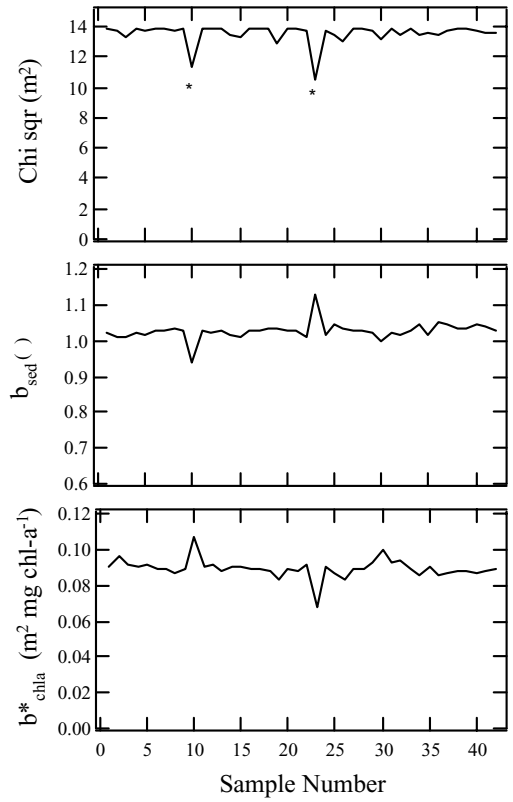

Figure 5. Detection of outliers (marked by *) using the Jackknife technique. (a) The sequence of values of Chi square; (b) the sequence of estimated values of unitless sediment scattering calibration multiplier b_{sed}; (c) the sequence of estimated values for b^*_{chl}. The original 41 data points were reduced to 39 points.

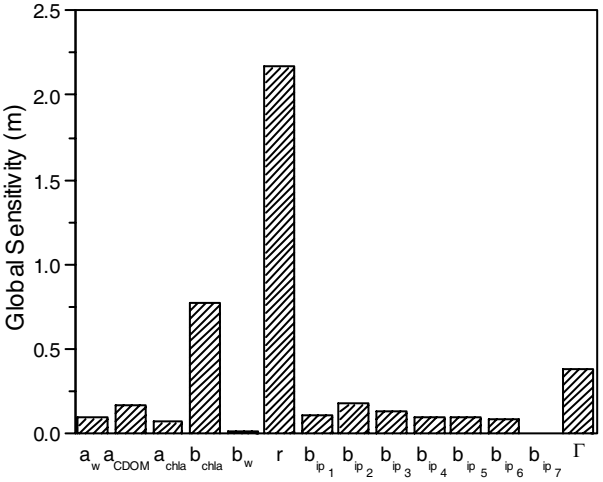

Figure 6. Results of sensitivity analysis for all model parameters following calibration. Sensitivity is measured in terms of change in modeled Secchi depth (m).

ed, estimation of the parameter uncertainty was accomplished by applying a bootstrapped Monte Carlo resampling method (Efron and Tibshirani, 1993; Meinrath et al., 2000). It provides an estimate of the uncertainty associated with the parameters' optimal values by generating a large number of pseudo-calibration sets (1000 in this case) by randomly selecting data points, with replacement, from the measured calibration set. Thus a data point may be present more than one time in one particular sample set or not present at all. The model is calibrating for each pseudo-calibration set, producing a distribution of parameter values. The empirical cumulative distribution function (CDF) is an estimate of the true but unknown distribution function of a parameter. The derivative of the CDF is the empirical probability density distribution (EDF) that provides a measure of parameter uncertainty (Meinrath et al., 2000).

Model calibration and validation

The model was calibrated and validated using data collected at the Index and Midlake stations (Fig. 1) throughout the year from 1999 to 2002. The available field data were split into two sets. One set (with $l = 21$ data) was used to calibrate parameter values, as described above, while the second set (with $p = 20$ data) was used for validation. Data were distributed such that all seasons, years, and sample stations were represented in both the calibration and validation sets. Particle and chlorophyll concentrations were trapezoidally depth-integrated for Index profiles from the surface to the observed Secchi depth. For Midlake profiles, the 0 and 10 m depth samples were averaged.

Using the fixed values (Table 2) and preliminary estimates of the adjustable parameters, outliers were identified. Figure 5 shows the results, whereby the original 40 data points were reduced to 39 (20 in the calibration set and 19 in the validation set). Dixon's test (Dixon, 1950) in combination with a Jackknife sampling method identified the two points as outliers. The value of Dixon's test changes dramatically when the two are removed (Fig. 5a). The two points correspond to large departures in estimated values for b_{sed} (Fig. 5b) and b^*_{chla} (Fig. 5c).

Calibration and validation results

Global sensitivity analysis identified which of the model coefficients had the largest effect on predicted Secchi depth. Each coefficient was varied by ±20 % with the exception of Γ, which was varied by ±5 %. Since Γ varies gradually as a function of water reflectivity and threshold contrast over their expected ranges, this smaller range captured the expected range of Γ itself. The most numerically sensitive coefficients were a_{CDOM}, b^*_{Chla}, r and Γ (Fig. 6). The values of a_{CDOM} and Γ were set to their mean measured and estimated values, respectively. The remaining two coefficients, b^*_{Chla} and r, were used as

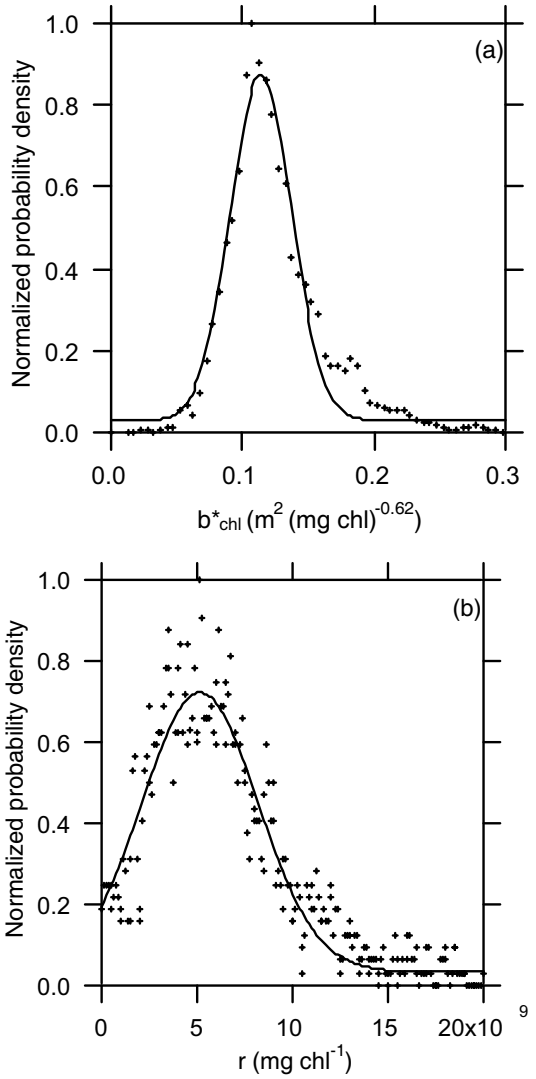

Figure 7. (a) Probability density function for b^*_{Chla}. The calibrated value is 0.105 m^2 $mg^{-0.62}$; the bootstrap estimated uncertainty is ± 0.07 m^2 $mg^{-0.62}$; (b) Probability density function for *r*: The calibrated value is 5.6 x 10^9 m^3 mg^{-1} and estimated uncertainty is 4 x 10^8 m^3 mg^{-1}.

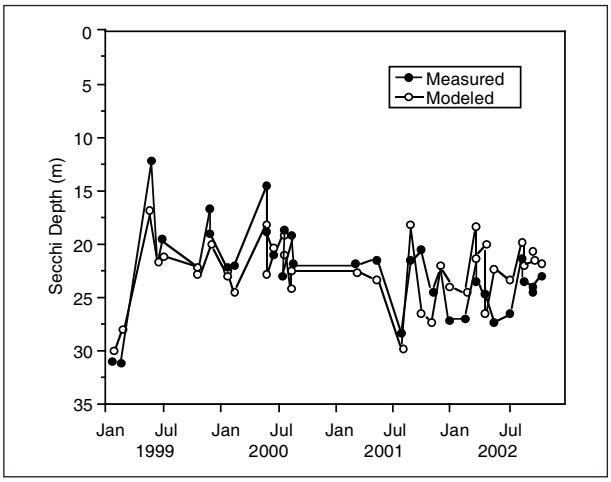

Figure 8. Predicted and measured Secchi Depth for all data available. r = 0.70. See Table 3 for summary statistics. Horizontal axis is days since 1 January 1999.

calibration parameters. The bootstrap analysis provided an estimate of uncertainty for the values of b^*_{Chla} and *r* (Fig. 7a, b).

The mean relative percent difference (RPD) between predicted and observed Secchi depth for the validation data set was –0.46 %, while the RPD over the four years was 7.9 % ± 8.3 % (mean ± s.d.; Table 3). The overall model performance, as reflected by the comparison of Secchi depth, is within the uncertainty associated with the hour-to-hour variations in Secchi depth. Comparing the measured and predicted Secchi depths for the calibration set yielded a correlation coefficient of R^2 = 0.48. A similar value (R^2 = 0.50) was obtained for the validation set. The slight difference is due to somewhat larger variability within the calibration data set. The entire data set is plotted in Figure 8 (R^2 = 0.49). The overall seasonal patterns were simulated, and in most cases, date-to-date trends were captured.

As an additional check of the model, and because K_d(PAR) is also of fundamental interest, we compared measured and predicted K_d for all available dates within the study period. K_d was measured at the Index station only, on 18 dates. The mean modeled K_d of 0.095 ± 0.0092 m^{-1} is very close to the mean observed K_d of 0.087 ± 0.011 m^{-1}. The dynamic range of K_d on the sampling dates used in the model was unfortunately narrow relative to the range of K_d values from the long-term monitoring program. For example, recent K_d values have been as low as 0.053 m^{-1}, observed on 25 April 1996 (corresponding Secchi depth was 41 m) during an upwelling event at the Index station.

Discussion

The model enables the quantitative evaluation of the various contributors to the Secchi depth within the range of conditions observed over the course of the study period. The percentage contributions to light attenuation in the calibration data set, caused by each of the primary parameters, is presented in Figure 9. As has often been found in other aquatic systems, light scattering is the dominant attenuant (Kirk, 1994; Mobley, 1994). The sensitivity analysis indicated that the scattering parameters associated with the organic and inorganic particulate fractions were also the dominant attenuants in Lake Tahoe, in which particulate scattering contributes between 70 and 80 % of attenuation. Approximately 58 % of attenuation is due, on average, to inorganic particles and 25 % due to organic particles. With few exceptions, the period of late spring

Table 3. Comparison of observed and modeled Secchi Depth as annual means. * indicates means are different at the 0.05 confidence level; ** indicates means are different at the 0.10 confidence level.

	Secchi Depth (m), mean ± std. dev.						
	Calibration Data Set	**Validation Data Set**	**All Data**	**Year 1999**	**Year 2000**	**Year 2001**	**Year 2002**
Observed	23.2 ± 4.7	21.7 ± 2.6	22.5 ± 3.8	21.9 ± 6.2	20.4 ± 2.6	22.6 ± 3.0	24.3 ± 2.0
Modeled	23.2 ± 3.8	21.6 ± 2.5	22.4 ± 3.2	22.5 ± 4.1	21.7 ± 1.9	23.8 ± 4.5	22.1 ± 2.8
RPD	0.00 %	–0.46 %	–0.44 %	2.74 %	6.37 % *	5.31 %	–9.05 % **

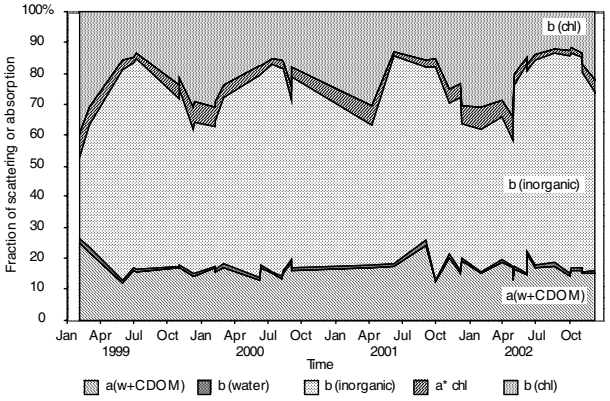

Figure 9. Modeled relative contribution (%) to the absorption and scattering of each modeled term due to each suspended matter type during the modeled period. The model is focused on 475 nm (see text).

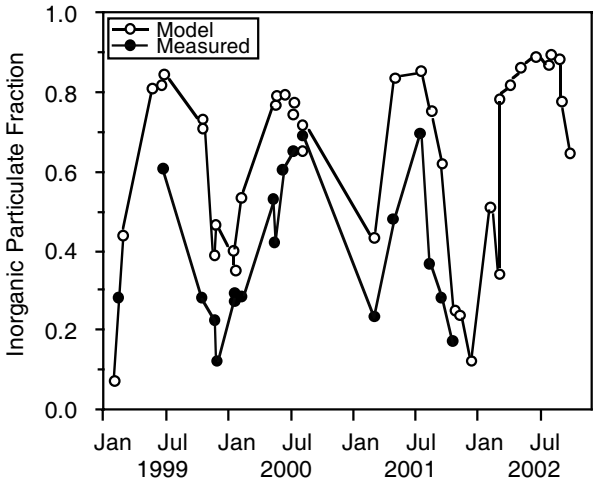

Figure 10. Comparison of the inorganic fraction of the total particle numbers, as given by measurements and the model. Horizontal axis is days since 1 January 1999. Note, measured values of inorganic particulate fraction were not available for all dates.

snowmelt exhibits an increase in inorganic particle scattering, contributing greater than 50 % of total attenuation. This is due to the high scattering efficiency of inorganic particles. Conversely, during autumn deep mixing and winter months, when stream flow is minimal, organic particle scattering and absorption is relatively larger. This winter deep mixing is the period in which the greatest Secchi depth clarity is observed.

The calibrated value for the chlorophyll scattering parameter, of b^*_{Chla} is higher than the values suggested previously by Morel (1987, 1994). The difference may be due to the fact that Morel's data came from Case 1 waters in which there was minimal inorganic sediment. (Case 1 waters (Morel and Prieur, 1977) are those in which the concentration of phytoplankton is high compared to non-biological particles. Case 1 has also come to mean that the optical properties are primarily determined by phytoplankton pigments. Case 2 waters have been referred to as "everything else" (Mobley, 1994), namely waters in which inorganic particles or dissolved organic matter dominate). This may have lead to a bias in the GA's estimated value of b^*_{Chla}.

The conversion factor r linking chlorophyll concentration to the number of organic particles has been identified as a highly sensitive model coefficient. The value of this fraction may be compared with a measured fraction, based on the SEM and X-ray particle elemental analysis described earlier (Fig. 10). This illustrates the observed seasonal patterns of relatively high inorganic fraction corresponding to late spring snowmelt. The increase in chlorophyll concentration during late autumn mixing (December) and winter deep mixing (Jan–April) is also clearly evident.

The model tends to over-predict the inorganic fraction by about 20 %. This may be due in part to the fact that the total particle numbers measured by the Liquilaz may be biased toward inorganic particles with high index of refraction, whereas algae with a lower index of refraction may be undercounted.

These findings appear to confirm Jassby et al. (1999) who, based on an analysis of a 30 year time series in Lake Tahoe, hypothesized that the Secchi minimum in May-June was most likely due to fine suspended sediment loading from the watershed, while the minimum in December was most likely due to mixed layer deepening as

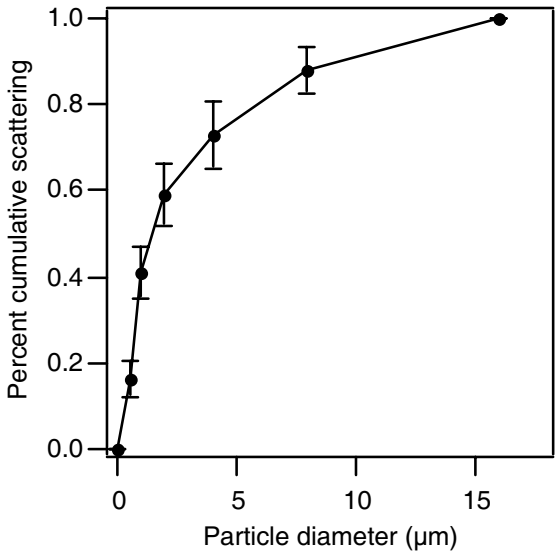

Figure 11. Cumulative contribution to the scattering coefficient, b_{ip}, for each of the particle size ranges. Due to the relative rarity of large particles, the scattering coefficient for the seventh size class (32–64 μm) was assigned to zero. Size range 1–6 correspond to 0.5–1, 1–2, 2–4, 4–8, 8–16, and 16–32 μm, respectively.

organic particles from the deep chlorophyll layer (typically 60 to 70 m deep in Lake Tahoe) are mixed upward into the Secchi stratum. The observations and laboratory analyses strongly bear out that hypothesis.

Given the importance of inorganic sediment particles to the clarity of Lake Tahoe, a more detailed analysis of the influence of particle size on Secchi depth is appropriate. In Figure 11, the part of the attenuation due to inorganic particle scattering is shown as a function of the particle size classes used in the model. As expected, due to the steeply sloped particle size distribution (Fig. 3), combined with greater scattering efficiency of relatively small particles (Eqns. 5 and 6) the majority of the scattering is due to the finest particle fractions, between 1 and 16 μm diameter, corresponding to the finest silts and clays. For inorganic particles, approximately 75 % of the scattering is due to particles between 0.5 and 5 μm (Fig. 11).

Detailed knowledge of particle concentration, PSD, and inorganic fraction is not generally available in most systems. We have found in the extreme case of Lake Tahoe that clarity is sensitive to these variables (Eqn. 1; see also Larson and Buktenica, (1998)). However, in systems of lower clarity, the principles presented here might be applied in simplified form.

Conclusions

We have found that both biological (e. g., phytoplankton and detritus) and inorganic (terrestrial sediment) particulate matter are important contributors to clarity loss in Lake Tahoe. The high scattering cross-section of inorganic particles results in their often being the dominant cause of loss of light transmission, despite their numerical minority most of the year. By coupling organic and inorganic suspensoid concentrations in the lake to a predicted Secchi depth, the model represents a useful tool that can be used to guide restoration efforts within the Tahoe basin, and other systems where clarity is a concern. By organizing the model around optical principles, the relative contributions of attenuants can be understood and further investigated in greater detail than would be possible with a simple regression model. Use of the model will guide further field and laboratory research, by pointing out the dominant attenuants and the importance of watershed and lake processes such as sediment erosion, nutrient transport and particle aggregation.

Specifically for Lake Tahoe, the model lends solid support to the earlier hypothesis (Jassby et al., 1999) that inorganic particles dominate clarity for most of the year, except in winter, when mixing of the deep chlorophyll layer results in greater attenuation by organic particles. Of the inorganic particles, it is the finer fraction (1–16 μm) that have the greatest impact on clarity.

The relative roles of organic and inorganic attenuants elucidated by the model have implications for Lake Tahoe restoration planning. Both biotic and abiotic particles contribute to clarity loss. However, as suggested by Jassby et al. (1999), because the attenuants differ in their causes and dynamic time scales, different restoration measures will apply to their reduction. The residence times of nutrients in Lake Tahoe are on the order of several decades (Jassby et al., 1995). The residence time of suspended inorganic particles may be much shorter, depending on size distribution, mechanisms of aggregation, and mixing. As predictions of inorganic particle fluxes from the watershed become available, the model will provide a linkage between erosion control measures and the lake's response.

Acknowledgments

We thank Prof. Emmanuel Boss and an anonymous reviewer for comments. We thank Robert C. Richards for advice, observations, and the sampling of more than 3000 L of water and Scott Hackley for chlorophyll analyses. We thank Steven C. Chapra for substantial comments on an earlier version of this manuscript. Jenny Coker initiated our study of particle size distribution, and laboratory analyses have been continued by Gandhi de Paz, Aaron O'Callaghan, Banu Sunman and Andrew Funk. We thank Deborah Hunter for sharing her extensive knowledge of the Lake Tahoe phytoplankton community and Patricia Arneson for assistance with data from the

Tahoe long-term monitoring program. This work was partially supported by the EPA, the U.S. EPA sponsored Center for Ecological Health Research (CEHR) at U.C. Davis, and grants 01-174-160-0 and 01-175-160-0 from the Lahontan Regional Water Quality Control Board. The research described has not been subjected to any EPA review and therefore does not necessarily reflect the views of the Agency, and no official endorsement should be inferred.

References

APHA, A. P. H. A., 1998. Standard Methods for the Examination of Water and Wastewater, 19th ed. American Public Health Association. 1540 pp.

Babin, M. and D. Stramski, 2004. Variations in the mass-specific absorption coefficient of mineral particles suspended in water. Limnol. Oceanogr. **49:** 756–767.

Beasley, D., D. R. Bull and R. R. Martin, 1993. An overview of genetic algorithms: Part 1, Fundamentals. University Computing **13:** 58–69.

Beckman, R. J. and R. D. Cook, 1983. Outliers. Technometrics **25:** 119–149.

Bevington, P. R. and D. K. Robinson, 1992. Data Reduction and Error Analysis for the Physical Sciences. McGraw-Hill. 328 pp.

Boss, E., M. S. Twardowski and S. Herring, 2001. Shape of the particulate beam attenuation spectrum and its inversion to obtain the shape of the particulate size distribution. Appl. Opt. **40:** 4885–4893.

Brun, R., M. Kuhni, H. Siegrist, W. Gujer and P. Reichert, 2002. Practical identifiability of ASM2d parameters – systematic selection and tuning of parameter subsets. Water Res. **36:** 4113–4127.

Brun, R., P. Reichert and H. R. Künsch., 2001. Practical identifiability analysis of large environmental simulation models. Water Resour. Res. **37:** 1015–1030.

Buiteveld, H., 1995. A model for calculation of diffuse light attenuation (PAR) and Secchi depth. Neth. J. of Aquat. Ecol.**29:** 55–65.

Buiteveld, H., J. H. M. Hakvoort and M. Donze, 1994. The optical properties of pure water. In: Ocean Optics XII. SPIE, pp. 174–178.

Bukata, R. P., J. H. Jerome, K. Y. Kondratyev and D. M. Pozdenyakov, 1995. Optical Properties and Remote Sensing of Inland and Coastal Waters. CRC Press. 362 pp.

Carlson, R. E., 1977. A trophic state index for lakes. Limnol. Oceanogr. **22:** 361–369.

Carroll, D. L., 1996. Chemical laser modeling with genetic algorithms. AIAA J. **34:** 338–346.

Coker, J. E., 2000. Optical Water Quality of Lake Tahoe. University of California, Davis.

Davies-Colley, R. J., W. N. Vant and D. G. Smith, 2003. Colour and Clarity of Natural Waters: Science and Management of Optical Water Quality. Blackburn Press. 310 pp.

Dirks, R. W. J., 1990. On the colour of the sea, with reference to remote sensing. Dissertation. Universität Utrecht, 206 pp.

Dixon, W. J., 1950. Analysis of extreme values. Ann. Math. Stat. **21:** 488–506.

Duntley, S. Q., 1952. The visibility of submerged objects. Visibility Lab., Mass. Inst. Tech. Summary Tech. Rept. Div., 74 pp.

Effler, S. W., R. K. Gelda, J. A. Bloomfield, Q. S. O. and D. L. Johnson, 2001. Modeling the effects of tripton on water clarity: Lake Champlain. J. Water Resour. Plan. Manage.-ASCE **127:** 224–234.

Effler, S. W. and M. Perkins, 1996. Optics, Chapter 7. In: S. W. Effler (ed.), Limnological and Engineering Analysis of a Polluted Urban Lake, New York. Springer Series on Environ. Manage.. Springer-Verlag, pp. 832.

Efron, B., 1979. 1977 Rietz Lecture - Bootstrap Methods – Another Look at the Jackknife. Ann. Stat. **7:** 1–26.

Efron, B. and R. Tibshirani, 1993. An Introduction to the bootstrap. Chapman and Hall. 436 pp.

Gardner, J. V., L. A. Mayer and J. E. H. Clarke, 2000. Morphology and processes in Lake Tahoe (California-Nevada). Geol. Soc. Am. Bull. **112:** 736–746.

Goldberg, D. E., 1989. Genetic Algorithms in search, optimization and machine learning. Addison-Wesley, 412 pp.

Goldman, C. R., 2000. Four decades of change in two subalpine lakes. Verh. Internat. Verein. Limnol. **27:** 7–26.

Gordon, H. R., 1989. Can the Lambert-Beer law be applied to the diffuse attenuation coefficient of ocean water? Limnol. Oceanogr. **34:** 1389–1409.

Gordon, H. R. and A. W. Wouters, 1978. Some relationships between Secchi depth and inherent optical properties of natural waters. Appl. Opt. **17:** 3341–3343.

Hakanson, L., 1995. Models to Predict Secchi Depth in Small Glacial Lakes. Aquat. Sciences **57:** 31–53.

Hakanson, L. and V. V. Boulion, 2003. A model to predict how individual factors influence Secchi depth variations among and within lakes. Int. Rev. Hydrobiol. **88:** 212–232.

Højerslev, N. K., 1986. Visibility of the sea with special reference to the Secchi disc. In: M. A. Blizard (ed.), Ocean Optics VIII, Proc. SPIE. Int. Soc. Opt. Eng. (SPIE). Bellingham, WA, pp. 294–305.

Hunter, D. A., C. R. Goldman and E. R. Byron, 1990. Changes in the phytoplankton community structure of Lake Tahoe, California-Nevada. Verh. Internat. Verein. Limnol. **24:** 505–508.

Hutchinson, G. E. and Y. H. Edmondson, 1957. A treatise on limnology. Wiley.

Jassby, A. D., C. R. Goldman and J. E. Reuter, 1995. Long-term change in Lake Tahoe (CA-NV, USA) and its relation to atmospheric deposition of algal nutrients. Arch. Hydrobiol. **135:** 1–21.

Jassby, A. D., C. R. Goldman, J. E. Reuter and R. C. Richards, 1999. Origins and scale dependence of temporal variability in the transparency of Lake Tahoe, California-Nevada. Limnol. Oceanogr. **44:** 282–294.

Jassby, A. D., J. E. Reuter, R. P. Axler, C. R. Goldman and S. H. Hackley, 1994. Atmospheric deposition of nitrogen and phosphorus in the annual nutrient load of Lake Tahoe (CA-NV). Water Resour. Res. **30:** 2207–2216.

Jewson, D. H., J. F. Talling, M. J. Dring, T. M. M., S. I. Heaney and C. Cunningham, 1984. Measurement of photosynthetically available radiation in freshwater: comparative tests of some current instruments used in studies of primary production. J. Plank. Res. **6:** 259–273.

Johnson, D. L., J. F. Jiao, S. G. Dossantos and S. W. Effler, 1991. Individual particle analysis of suspended materials in Onondaga Lake, New-York. Envir. Sci. Tech. **25:** 736–744.

Junge, C. E., 1963. Air Chemistry and Radioactivity, Academic. 382 pp.

Kirk, J. T. O., 1994. Light and Photosynthesis in Aquat. Ecosystems, 2 ed. Cambridge. 509 pp.

Knollenberg, R. G., 1987. The importance of media refractive-index in evaluating liquid and surface microcontamination measurements. J. Envir. Sci. **30:** 50–58.

Larson, G. L. and M. W. Buktenica, 1998. Variability of Secchi disk readings in an exceptionally clear and deep caldera lake. Arch. Für Hydrobiol. **141:** 377–388.

Levin, I. M., E. Desa, E. Desa, T. Suresh and T. Radomyslskaya, 2000. Can the Secchi depth measurements be used for determination of water inherent optical properties? In: Ocean Optics, St. Petersberg, pp. 63–73.

Levin, I. M. and T. Radomyslskaya, 2000. Refined Secchi depth theory: On Preisendorfer's criticism of determining water at-

tenuation coefficient through Secchi depth measurements. In: Phys. Proc. in Nat. Waters, pp. 63–67.
Marjanovic, P., 1989. Mathematical modeling of eutrophication processes in Lake Tahoe: water budget, nutrient budget and model development. U. California, Davis, CA.
Meinrath, G., C. Ekberg, A. Landgren and J. O. Liljenzin, 2000. Assessment of uncertainty in parameter evaluation and prediction. Talanta **51:** 231–246.
Mitchell, B. G., 1990. Algorithms for determining the absorption coefficient of aquatic particulates using the quantitative filter technique (QTF). In: R. W. Spinrad (ed.), Ocean Optics X. SPIE. pp. 137–148.
Mobley, C. D., 1994. Light and Water: Radiative Transfer in Natural Waters. Academic. 592 pp.
Morel, A., 1974. Optical Properties of Pure Water and Pure Sea Water. In: N. G. Jerlov and E. S. Nielsen (eds.), Optical Aspects of Oceanography, Academic Press, London, pp. 1–24.
Morel, A., 1987. Chlorophyll-specific scattering coefficient of phytoplankton – a simplified theoretical approach. Deep-Sea Res. A **34:** 1093–1105.
Morel, A., 1994. Optics from the single cell to the mesoscale. In: R. W. Spinrad, K. L. Carder and M. J. Perry (eds.), Ocean Optics. Oxford Monogr. Geol. Geophys., Oxford U. Press, pp. 93–106.
Morel, A. and L. Prieur, 1977. Analysis of variations in ocean color. Limnol. Oceanogr. **22:** 709–722.
Mueller, J. L. and G. S. Fargion, 2002. Ocean Optics Protocols For Satellite Ocean Color Sensor Validation, Revision 3. NASA. 308 pp.
Omlin, M., R. Brun and P. Reichert, 2001. Biogeochemical model of Lake Zurich: Sensitivity, identifiability and uncertainty analysis. Ecol. Mod. **141:** 105–123.
Perez-Losada, J., 2001. A Deterministic Model for Lake Clarity. Application to Lake Tahoe (California, Nevada), USA. U. Girona, Spain. 233 pp.
Pope, R. M. and E. S. Fry, 1997. Absorption spectrum (380–700 nm) of pure water. II. Integrating cavity measurements. Appl. Opt. **36:** 8710–8723.
Preisendorfer, R. W., 1986a. Eyeball optics of natural waters: Secchi disk science. Pacific Mar. Envir. Lab., Seattle WA. 90 pp.
Preisendorfer, R. W, 1986b. Secchi disk science: Visual optics of natural waters. Limnol. Oceanogr. **31:** 909–926.
Smith, R. C., J. E. Tyler and C. R. Goldman, 1973. Optical properties and color of Lake Tahoe and Crater Lake. Limnol. Oceanogr. **18:** 189–199.
Stedmon, C. A., S. Markager and H. Kaas, 2000. Optical properties and signatures of chromophoric dissolved organic matter (CDOM) in Danish coastal waters. Estuar. Coast. Shelf Sci. **51:** 267–278.
Swift, T. J., 2004. The aquatic optics of Lake Tahoe, CA-NV. University of California Davis. 212 pp.
Tassan, S. and G. M. Ferrari, 1995. Proposal for the measurement of backward and total scattering by mineral particles suspended in water. Appl. Opt. **34:** 8345–8353.
Tilzer, M. M., 1988. Secchi disk – chlorophyll relationships in a lake with highly variable phytoplankton biomass. Hydrobiol. **162:** 163–171.
Tyler, J. E., 1968. The Secchi disc. Limnol. Oceanogr. **13:** 1–6.
van de Hulst, H. C., 1957. Light scattering by small particles. John Wiley, New York, 470 pp.
Van Duin, E. H. S. and others 2001. Modeling underwater light climate in relation to sedimentation, resuspension, water quality and autotrophic growth. Hydrobiol. **444:** 25–42.
Vant, W. N. and R. J. Davies-Colley, 1984. Factors affecting clarity of New-Zealand lakes. N. Z. J. Mar. Freshw. Res. **18:** 367–377.
Weidemann, A. D. and T. T. Bannister, 1986. Absorption and scattering coefficients in Irondequoit Bay. Limnol. Oceanogr. **31:** 567–583.
Yin, C. Q. and D. L. Johnson, 1984. An individual particle analysis and budget study of Onondaga Lake-sediments. Limnol. Oceanogr. **29:** 1193–1201.